International Journal of Engineering

Journal Homepage: www.ije.ir

Numerical Simulation of Frost Formation in Interrupted Micro Channel Heat Sinks Considering Microfluidic Effects in Slip Regime

H. Safikhani*, H. Shaabani

Department of Mechanical Engineering, Faculty of Engineering, Arak University, Arak, Iran

PAPER INFO

Paper history:
Received 18 August 2020
Received in revised form 06 September 2020
Accepted 09 September 2020

Keywords:
Micro Channels Heat sinks
Microchannel
Frost Formation
Computational Fluid Dynamics
Slip Regime
Microfluidic

ABSTRACT

Frost formation is a renowned phenomenon in HVAC, aeronautical and refrigeration industries. In this paper, numerical modeling and parametric study of the frost formation in the interrupted Micro Channels Heat sinks (MCHS) is investigated considering microfluidic effects in slip flow regime. For numerical modeling, basic equations of humid air and frost including continuum, momentum, energy and phase change mechanism are numerically solved and results are compared with reported data. Knudsen number (Kn) is changed so that slip flow regime requirement is accomplished. This requirement is also considered for setting boundary conditions. The effect of different parameters like cold surface temperature, time and Kn are studied on the frost formation and details of the flow field. Results revealed that with an increase in time and a decrease in Kn and cold surface temperature, weight and thickness of the frost increase. Moreover, with thicker frost maximum flow velocity rises in the microchannel. The details of frost formation and flow field, revealed by the numerical results can remarkably assist designing interrupted microchannel.

***doi**: 10.5829/ije.2020.33.12c.17*

1. INTRODUCTION

Frost formation is a renowned phenomenon in HVAC, aeronautical and refrigeration industries. Frost mounting on the heat exchanger surfaces, causing higher thermal resistance and also it blocks the air path. Both phenomena decrease energy efficiency of the system. Frost naturally is a porous media with packs of the air trapped in the ice matrix. Therefore, it possesses a marked thermal resistance. The presence of frost in the heat exchanger's channels causes pressure drop with narrowing down the path of the air. In the process of the frost formation, humid flows pass coolant surface and mass transfer of steam present in the wet flow to the ice crystals when the air is saturated. This causes thicker frost and higher freezing density. Many researchers already have studied frost formation by numerical and experimental approaches. Hayashi et al. [1] was one of the pioneers who studied the growth of frost in three different time periods. The first period includes the primary initiation of the ice crystals which is quite short in comparison of the total time period. In this period frost does not grow markedly thick. Moreover, for this phase, it is not a porous media as it can be assumed as ice idols where convection heat and mass transfer are main growth mechanisms and diffusion to the frost sounds trivial. For the second period known as frost growth phase, frost is a porous media where molecular diffusion of the water vapor is dominant. Mass flow of the water vapor contributed in both increasing the density of the frost as well as growing it. Finally, in the complete growth period of the frost, the temperature of the freezing surface reaches to water triple-point temperature. Therefore, a cyclic process starts where compressed water vapor diffuses through the frost and gradually freezes due to internal temperature gradient. Aoki et al. [2] thoroughly investigated this phase. Modeling frost formation can be classified in analytical models and computational fluid dynamics (CFD) based models. Analytical models generally assume the growth of the frost in only one

*Corresponding Author Institutional Email: *h-safikhani@araku.ac.ir* (H. Safikhani)

Please cite this article as: H. Safikhani, H. Shaabani, Numerical Simulation of Frost Formation in Interrupted Micro Channel Heat Sinks Considering Microfluidic Effects in Slip Regime, International Journal of Engineering, Transactions C: Aspects Vol. 33, No. 12, (2020), 2556-2562.

direction. Tao et al. [3, 4] proposed a model for mass transfer in frost layer. Lee et al. [5, 6] presented a uni-dimensional model for simulating growth in frost density and thickness and also they developed a model for analyzing frost layer and air flow. Using averaging local volume method Le Gall et al. [7] introduced the relative equilibrium to anticipate frost growth. Na and Webb [8-10] suggested a model based on density of supersaturated water vapor in the frost layer. Yang et al. [11] found an effective model to prognosticate the performance of the fin-tube heat exchanger. Recently, Hermes et al. [12] developed a mathematical model which could accurately predict the frost thickness with a 10% discrepancy with experimental results. Kandula [13, 14] proposed novel equations for frost over the straight surface and investigated the effect of different ambient parameters on frost characteristics.

Micro-channel heat exchangers are very efficient compact exchangers. Their benefit in comparison with fin-tube exchangers includes lower volume and weight and higher efficiency. They also possess lower internal space which decreases refrigeration load of the exchanger and potentially decreases the contribution in global warming with lower possible leakage of the refrigerant [15]. Lately, micro-channel exchangers are prevalent in HVAC systems. These exchangers are increasingly applied in chillers especially thermal pumps where they should work in wet and freezing condition. Shao et al. [16] studied a model with distributed micro-channel exchangers used in commercial thermal pumps to analyze the frost over the fin-tube evaporators. Moallem et al. [17, 18] investigated the effect of surface temperature, surface coating and water blockage on the freezing performance of the micro-channel heat exchangers. Surface temperature was more important than surface coating and water blockage over frost growth speed and freezing time. Some other studies focused on the frost-defrost cycle of the heat exchangers which is very vital in designing thermal pump systems. Xia et al. [19] studied five different louvered-fin micro-channel heat exchangers and found that condensed droplets dramatically influence the pressure drop and heat transfer in recurring freezing cycles. Zhang and Hrnjak [20] studied the freezing performance of the micro-channel heat exchangers with parallel-flow parallel-fin (PF2) horizontal flat tubes. In comparison with conventional serpentine fins, the freezing performance was improved which is attributed to the superior permeability of the PF2 exchangers. Tso et al. [21] developed a distribution model taking into account the non-uniform distribution of the wall and air temperature in the coil to anticipate dynamic behavior of the finned-tube heat exchanger for both frost and non-frost conditions. Wu et al. [22] studied the frost properties of a micro-channel exchanger with louvered-fin and derived the equation for the thickness of the frost. In recent years, Zhu et al. [23, 24] concentrated on increasing thermal transfer through the concept of reconstruction of developed thermal layers. This study included some parallel longitudinal micro-channels with some transverse channels. The transverse channels were used to divide the length of the flow into some independent streams. They found that computed hydraulic and thermal boundary layers were readily improved due to the shorter total length of the divided streams within the micro-channel. In addition, it was that the pressure drop and also heat transfer improved in divided micro-channels in comparison with conventional micro-channels. In another similar study Cheng [25] analyzed the flow and heat transfer of a double accumulated micro-channel using some micro-processor. The effect of height of the fin's wall to the height of the micro-channel was examined. They found their superior performance compared to the conventional micro-channels. The evaluation of the 3D micro-channels divided with the transverse micro-pores was followed by Chai et al. [26] using experimental and numerical methods. They found the pressure drop and heat transfer for different conditions and geometries of rectangular walls in transverse micro-pores. Wang and Li [27] numerically simulated flow field in micro-channels with triangular walls in transverse micro-pores. Their parametric studies eventuated in an optimized micro-channel with promising performance. Hajmohammadi et al. [28] investigated the slip regime in microchannel heat sinks with one phase flow. They finally compared the results with the related results without slip regime. To the best of author's knowledge, there has been no study focusing on the numerical modeling of the frost in micro channels considering the micro-fluidic effects in slip regime. Therefore, such an issue is the aim of this paper.

2. MATHEMATICAL MODELING

The details of numerical modeling is described in this section.

2. 1. Geometry The geometry investigated in this paper has been schematically illustrated in Figure 1. As is shown in this figure, a number of parallel domains

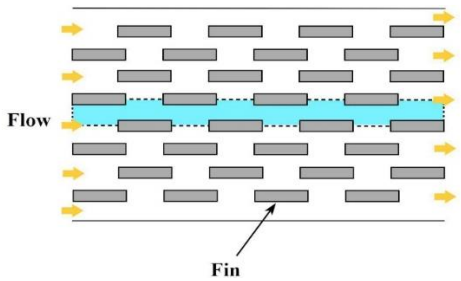

Figure 1. The schematic of geometry

have been placed next to each other and formed a MCHS. Since, in this MCHS, the flow field in each computational domain is the same, the governing equations have been numerically solved for one domain and finally, the amount of heat transfer from total MCHS have been multiplied by the number of domains to get the total values. The total pressure drop and heat transfer for the set of MCHS are computed as follows:

$$Q_{tot} = nQ_1 \quad (1)$$

$$\Delta P_{tot} = \Delta P_1 \quad (2)$$

$$n = \frac{W}{2(c+2a)} \quad (3)$$

In this paper, the basic dimensions of the MCHS (W and L) are constant and equal to 5 mm, while channel width (D) is 160 μm. In this way, the examined channels are classified as microchannels ($10\,\mu m < D \leq 200\,\mu m$). Other geometrical and non-geometrical parameters are shown in Table 1 and Figure 2.

2. 2. Governing Equations In the present CFD modeling it is assumed that humid air is treated as an incompressible Newtonian fluid in laminar flow and density (ρ_a), mass diffusivity coefficient (D_a) and specific heat capacity (c_{pa}) of air are constant. Natural convection is negligible in both humid air and frost. Moreover, the humid air within the frost layer is considered saturated [13, 29]. The continuity, 2D momentum, energy and mass transport equations are as follows:

$$\frac{\partial \rho_a}{\partial t} + \frac{\partial (\rho_a u)}{\partial x} + \frac{\partial (\rho_a v)}{\partial y} = 0 \quad (4)$$

TABLE 1. Geometrical and non-geometrical parameters

Parameter	Value
Half of fin thickness (a)	20 μm
Fin length (b)	225 μm
Half of channel width (c)	80 μm
Chip length (L)	5 mm
Chip width (W)	5 mm
Inlet velocity	0.1 $^m/_S$
Kn	0, 0.05, 0.1
Time	5, 10, 15 Min
Cold wall temperature	-15, -10, -5 ℃

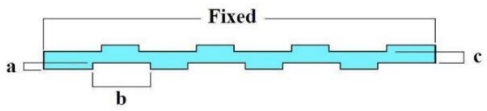

Figure 2. Geometrical parameters

$$\frac{\partial (\rho_a u)}{\partial t} + \frac{\partial (\rho_a u.u)}{\partial x} + \frac{\partial (\rho_a v.u)}{\partial y} = -\frac{\partial P}{\partial x} + \frac{\partial}{\partial x}\left(\mu \frac{\partial u}{\partial x}\right) + \frac{\partial}{\partial y}\left(\mu \frac{\partial u}{\partial y}\right) \quad (5)$$

$$\frac{\partial (\rho_a v)}{\partial t} + \frac{\partial (\rho_a u.v)}{\partial x} + \frac{\partial (\rho_a v.v)}{\partial y} = -\frac{\partial P}{\partial y} + \frac{\partial}{\partial x}\left(\mu \frac{\partial v}{\partial x}\right) + \frac{\partial}{\partial y}\left(\mu \frac{\partial v}{\partial y}\right) \quad (6)$$

$$\frac{\partial (\rho_a T)}{\partial t} + \frac{\partial (\rho_a u.T)}{\partial x} + \frac{\partial (\rho_a v.T)}{\partial y} = \frac{\partial}{\partial x}\left(\frac{\lambda_a}{C_{p,a}} \frac{\partial T}{\partial x}\right) + \frac{\partial}{\partial y}\left(\frac{\lambda_a}{C_{p,a}} \frac{\partial T}{\partial y}\right) \quad (7)$$

$$\frac{\partial (\rho_a w)}{\partial t} + \frac{\partial (\rho_a u.w)}{\partial x} + \frac{\partial (\rho_a v.w)}{\partial y} = \frac{\partial}{\partial x}\left(\rho_a D_a \frac{\partial w}{\partial x}\right) + \frac{\partial}{\partial y}\left(\rho_a D_a \frac{\partial w}{\partial y}\right) \quad (8)$$

Using an energy balance for a differential frost volume in the interior of the frost layer, energy equation can be expressed as:

$$\frac{\partial (\rho_f T)}{\partial_t} = \frac{\partial}{\partial x}\left(\frac{\lambda_f}{c_{p,f}} \frac{\partial T}{\partial x}\right) + \frac{\partial}{\partial y}\left(\frac{\lambda_f}{c_{p,f}} \frac{\partial T}{\partial y}\right) + \frac{q_{sub}}{c_{pf}} \frac{\partial \rho_f}{\partial t} \quad (9)$$

For the densification rate of frost layer, the equation proposed by Na and Webb [9] has been used:

$$\frac{\partial \rho_f}{\partial t} = \frac{\partial}{\partial x}\left(\rho_a D_{ef} \frac{\partial w}{\partial x}\right) + \frac{\partial}{\partial y}\left(\rho_a D_{ef} \frac{\partial w}{\partial y}\right) \quad (10)$$

The viscosity and thermal conductivity are considered to be temperature dependent. The thermal conductivity of frost is commonly expressed as a function of frost density. In this study, it is used a correlation reported by Lee et al. [6]:

$$\lambda_f \left[{}^{W}/_{(m.K)^{-1}}\right] = A_1 + A_2 \rho_f + A_3 \rho_f^2 \left[\rho \text{ in } {}^{kg}/_{m^3}\right] \quad (11)$$

where $A_1 = 0.132$ $A_2 = 3.13 \times 10^{-4}$ and $A_3 = 1.6 \times 10^{-7}$. The specific heat is defined as a function of frost density and porosity, as follows:

$$c_{p,f} = \frac{(c_{p,f}\rho_g(1-\varepsilon) + c_{p,a}\rho_a \varepsilon)}{\rho_f}. \quad (12)$$

The diffusive mass coefficient in the frost layer is determined as Na and Webb [8]:

$$D_{ef} = D_a \varepsilon^{\frac{1+\varepsilon}{2}}. \quad (13)$$

2. 3. Boundary and Initial Conditions For numerical simulation, the equations of previous sections should be solved subject to the related boundary and initial conditions. The schematic subjected boundary conditions are shown in Figure 3. The fluid entered to the channel with known velocity and temperature (inlet) and exited with the known pressure (outlet). The fins are walls with known temperature lower than freezing temperature. The slip 1st order boundary conditions (0.001<Kn<0.1) are investigated for walls. This study

models the frost layer growth period while the effects of crystal growth period are treated as initial conditions. Initial frost layer temperature is assumed to be constant and equal to the plate temperature, since the initial thickness is sufficiently thin.

2. 4. Numerical Methods Numerical simulation is performed using finite volume method. A second order upwind method is used for the convective and diffusive terms and the SIMPLE algorithm is employed to solve the coupling between the velocity and pressure fields. To make sure that the results are independent of the size and the number of generated grids, several grids with different sizes along different directions has been tested for each MCHS; and it has been attempted to consider for each one the best grid, with the highest accuracy and the lowest computation cost. A sample of generated grid is shown in Figure 4.

2. 5. Validation To validate the numerical model, its finding is compared with reliable results reported in related references. Since, there is neither experimental nor numerical study available on the frost formation in micro channels considering microfluidic effect in slip regime each frost formation and microfluidic effect should be evaluated separately. Figure 5 compares the results of frost formation in a conventional macro channel with that of Wu et al. [22]. As can be seen from Figure 5, present modeling is able to accurately simulate the frost formation. Similarly, Figure 6 shows the effect of slip effects in a micro-channel developed in this study with that of Hajmohammadi et al. [28] with one phase which reveals great correlation. Therefore, it can be said that presented model is accurate and reliable for simulation of frost formation in micro-channels considering microfluidic effects.

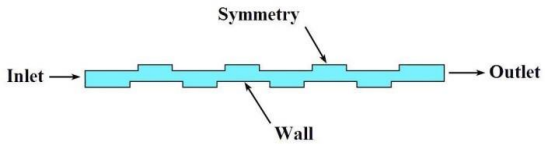

Figure 3. The schematic subjected boundary conditions

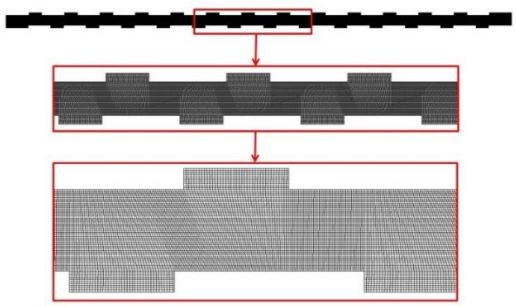

Figure 4. Sample of grid generation

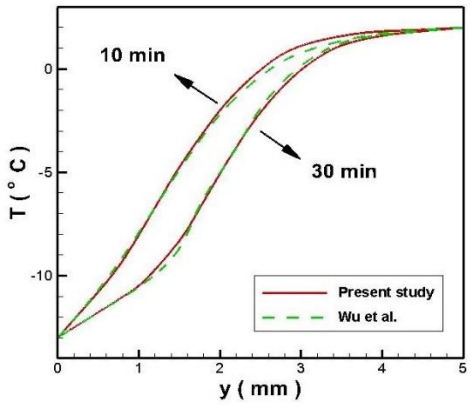

Figure 5. Validation of the model predictions of the frost formation

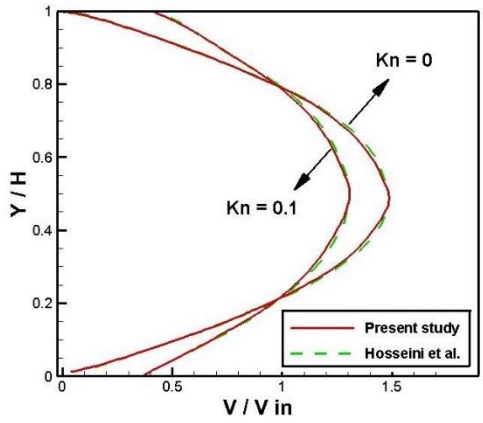

Figure 6. The effect of slip conditions in a micro-channel

3. RESULTS AND DISCUSSION

The effect of different parameters like time, cold wall temperature and Kn number on the growth of the frost and flow field are discussed in this section.

Frost formation is studied in three different time periods of 5, 10 and 15 minutes. Figure 7 illustrates the volume fraction contour of humid air with the time passing by. As can be observed from Figure 7, with increasing time from 5 to 15 minutes the growth of the frost speeded up and minimum volume fraction of humid air decreases from 0.7 to 0.3 which shows the frost growth with time increasing. Figure 8 depicts the velocity contour of the humid air with time corresponding to the higher frost growth. It can be inferred that until 15 minutes of time there is no discernable change in air velocity and it is probable that with a longer time period the air path becomes blind.

Similarly, frost formation is studied in three different cold wall temperatures of -15, -10 and -5 ^{o}C. Figure 9 illustrates the volume fraction contour of humid air with the cold wall temperature changing. As can be observed

from Figure 9, with decreasing cold wall temperature from -5 to -15 ºC, the growth of the frost speeds up and minimum volume fraction of humid air decreases from 0.9 to 0.2 which shows the frost growth with decreasing of cold wall temperature. Figure 10 depicts the velocity contour of the humid air with cold wall temperature. It can be inferred that as the cold wall temperature decreases, maximum humid air velocity increases due to growth in frost formation and narrowing of the air passage.

Three different Kn numbers 0, 0.05 and 0.1 is examined to analyze frost formation. Figure 11 shows the humid air volume fraction contour with different Kn numbers which reveals that with higher Kn number, lower growth of the frost occurs. Figure 12 shows the

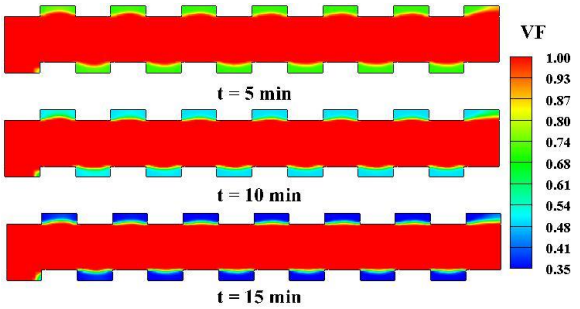

Figure 7. The volume fraction contour of humid air with the time passing

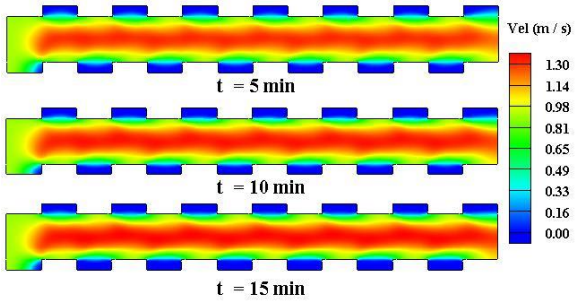

Figure 8. The velocity contour of humid air with the time passing

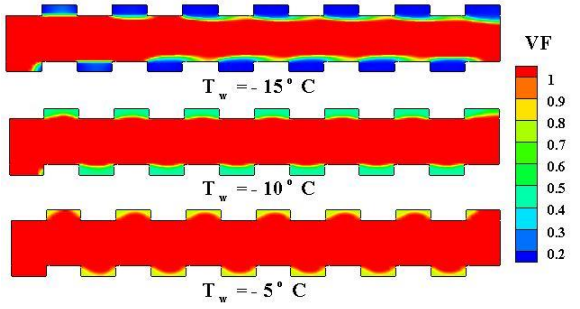

Figure 9. The volume fraction contour of humid air with the cold wall temperature changing

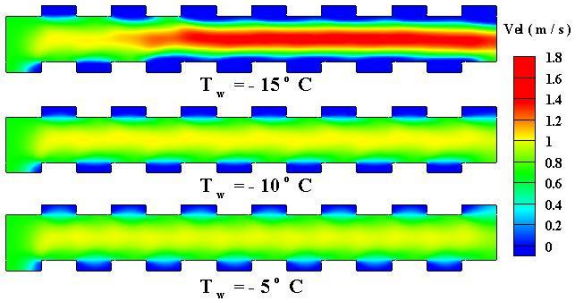

Figure 10. The velocity contour of humid air with the cold wall temperature changing

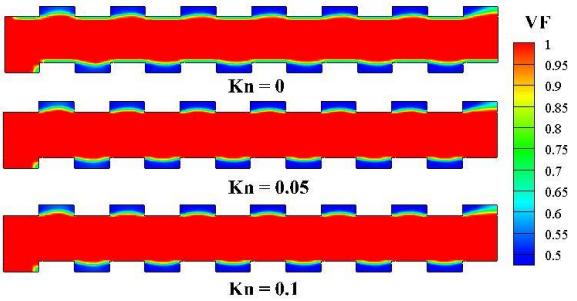

Figure 11. The humid air volume fraction contour with different Kn number

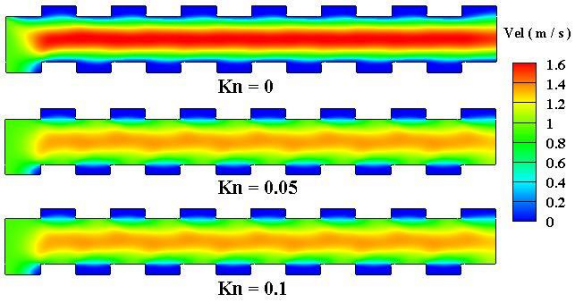

Figure 12. The humid air velocitycontour with different Kn number

humid air velocity contour with increasing Kn number corresponding to the frost reduction. As can be observed with Kn number equal to 0, which corresponds to non-slipping condition, air flow velocity is maximized.

4. CONCLUSION

In this paper, numerical modeling and parametric study of the frost formation in the interrupted MCHS was investigated considering microfluidic effects in slip flow regime. For numerical modeling, basic equations of humid air and frost including: continuum, momentum, energy and phase change mechanism were numerically solved. Kn number was changed so that slip flow regime

requirement was accomplished. This requirement was also considered for setting boundary conditions. The effect of different parameters like cold surface temperature, time and Kn were studied on the frost formation and details of the flow field. Results revealed that with an increase in time and a decrease in Kn and cold surface temperature, weight and thickness of the frost increase. The details of frost formation and flow field, revealed by the numerical results can remarkably assist designing interrupted microchannels.

5. REFRENCES

1. Hayashi, Y., Aoki, A., Adachi, S. and Hori, K., "Study of frost properties correlating with frost formation types", ***Journal of Heat Transfer***, Vol. 99, (1977), 239-245. doi:10.1115/1.3450675.
2. Aoki, K., Katayama, K. And Hayashi, Y., "A study on frost formation: The process of frost formation involving the phenomena of water permeation and freezing", ***Bulletin of JSME***, Vol. 26, No. 211, (1983), 87-93. https://doi.org/10.1299/jsme1958.26.87.
3. Tao, Y.-X., Besant, R. and Rezkallah, K., "Modeling of frost formation in a fibrous insulation slab and on an adjacent cold plate", ***International Communications in Heat and Mass Transfer***, Vol. 18, No. 5, (1991), 609-618. https://doi.org/10.1016/0735-1933(91)90074-E.
4. Tao, Y.-X., Besant, R. and Rezkallah, K., "A mathematical model for predicting the densification and growth of frost on a flat plate", ***International Journal of Heat and Mass Transfer***, Vol. 36, No. 2, (1993), 353-363. https://doi.org/10.1016/0017-9310(93)80011-I.
5. Lee, K.-S., Kim, W.-S. and Lee, T.-H., "A one-dimensional model for frost formation on a cold flat surface", ***International Journal of Heat and Mass Transfer***, Vol. 40, No. 18, (1997), 4359-4365. https://doi.org/10.1016/S0017-9310(97)00074-4.
6. Lee, K.-S., Jhee, S. and Yang, D.-K., "Prediction of the frost formation on a cold flat surface", ***International Journal of Heat and Mass Transfer***, Vol. 46, No. 20, (2003), 3789-3796. https://doi.org/10.1016/S0017-9310(03)00195-9.
7. Le Gall, R., Grillot, J. and Jallut, C., "Modelling of frost growth and densification", ***International Journal of Heat and Mass Transfer***, Vol. 40, No. 13, (1997), 3177-3187 . https://doi.org/10.1016/S0017-9310(96)00359-6.
8. Na, B. and Webb, R.L., "Mass transfer on and within a frost layer", ***International Journal of Heat and Mass Transfer***, Vol. 47, No. 5, (2004), 899-911. https://doi.org/10.1016/j.ijheatmasstransfer.2003.08.023.
9. Na, B. and Webb, R.L., "New model for frost growth rate", ***International Journal of Heat and Mass Transfer***, Vol. 47, No. 5, (2004), 925-936. https://doi.org/10.1016/j.ijheatmasstransfer.2003.09.001.
10. Na, B. and Webb, R.L., "A fundamental understanding of factors affecting frost nucleation", ***International Journal of Heat and Mass Transfer***, Vol. 46, No. 20, (2003), 3797-3808. https://doi.org/10.1016/S0017-9310(03)00194-7.
11. Yang, D.-K., Lee, K.-S. and Song, S., "Modeling for predicting frosting behavior of a fin–tube heat exchanger", ***International Journal of Heat and Mass Transfer***, Vol. 49, No. 7-8, (2006), 1472-1479. https://doi.org/10.1016/j.ijheatmasstransfer.2005.09.022.
12. Hermes, C.J., Piucco, R.O., Barbosa Jr, J.R. and Melo, C., "A study of frost growth and densification on flat surfaces", ***Experimental Thermal and Fluid Science***, Vol. 33, No. 2, (2009), 371-379. https://doi.org/10.1016/j.expthermflusci.2008.10.006.
13. Kandula, M., "Frost growth and densification in laminar flow over flat surfaces", ***International Journal of Heat and Mass Transfer***, Vol. 54, No. 15-16, (2011), 3719-3731.https://doi.org/10.1016/j.ijheatmasstransfer.2011.02.056.
14. Kandula, M., "Correlation of water frost porosity in laminar flow over flat surfaces", ***Special Topics & Reviews in Porous Media: An International Journal***, Vol. 3, No. 1, (2012), 79-87. DOI: 10.1615/SpecialTopicsRevPorousMedia.v3.i1.70
15. Garimella, S., "Innovations in energy efficient and environmentally friendly space-conditioning systems", ***Energy***, Vol. 28, No. 15, (2003), 1593-1614. https://doi.org/10.1016/S0360-5442(03)00120-8.
16. Shao, L.-L., Yang, L. and Zhang, C.-L., "Comparison of heat pump performance using fin-and-tube and microchannel heat exchangers under frost conditions", ***Applied Energy***, Vol. 87, No. 4, (2010), 1187-1197. https://doi.org/10.1016/j.apenergy.2009.08.021.
17. Moallem, E., Padhmanabhan, S., Cremaschi, L. and Fisher, D.E., "Experimental investigation of the surface temperature and water retention effects on the frosting performance of a compact microchannel heat exchanger for heat pump systems", ***International Journal of Refrigeration***, Vol. 35, No. 1, (2012), 171-186. https://doi.org/10.1016/j.ijrefrig.2011.08.010.
18. Moallem, E., Cremaschi, L., Fisher, D.E. and Padhmanabhan, S., "Experimental measurements of the surface coating and water retention effects on frosting performance of microchannel heat exchangers for heat pump systems", ***Experimental Thermal and Fluid Science***, Vol. 39, No., (2012), 176-188. https://doi.org/10.1016/j.expthermflusci.2012.01.022.
19. Xia, Y., Zhong, Y., Hrnjak, P.S. and Jacobi, A.M., "Frost, defrost, and refrost and its impact on the air-side thermal-hydraulic performance of louvered-fin, flat-tube heat exchangers", ***International Journal of Refrigeration***, Vol. 29, No. 7, (2006), 1066-1079. https://doi.org/10.1016/j.ijrefrig.2006.03.005.
20. Zhang, P. and Hrnjak, P.S., "Air-side performance of a parallel-flow parallel-fin (pf2) heat exchanger in sequential frosting", ***International Journal of Refrigeration***, Vol. 33, No. 6, (2010), 1118-1128. https://doi.org/10.1016/j.ijrefrig.2010.04.011.
21. Tso, C., Cheng, Y. and Lai, A., "An improved model for predicting performance of finned tube heat exchanger under frosting condition, with frost thickness variation along fin", ***Applied Thermal Engineering***, Vol. 26, No. 1, (2006), 111-120. https://doi.org/10.1016/j.applthermaleng.2005.04.009.
22. Wu, J., Ouyang, G., Hou, P. and Xiao, H., "Experimental investigation of frost formation on a parallel flow evaporator", ***Applied Energy***, Vol. 88, No. 5, (2011), 1549-1556. https://doi.org/10.1016/j.apenergy.2010.11.006.
23. Xu, J., Gan, Y., Zhang, D. and Li, X., "Microscale heat transfer enhancement using thermal boundary layer redeveloping concept", ***International Journal of Heat and Mass Transfer***, Vol. 48, No. 9, (2005), 1662-1674. https://doi.org/10.1016/j.ijheatmasstransfer.2004.12.008.
24. Xu, J., Song, Y., Zhang, W., Zhang, H. and Gan, Y., "Numerical simulations of interrupted and conventional microchannel heat sinks", ***International Journal of Heat and Mass Transfer***, Vol. 51, No. 25-26, (2008), 5906-5917. https://doi.org/10.1016/j.ijheatmasstransfer.2008.05.003.
25. Cheng, Y., "Numerical simulation of stacked microchannel heat sink with mixing-enhanced passive structure", ***International Communications in Heat and Mass Transfer***, Vol. 34, No. 3,

(2007), 295-303. https://doi.org/10.1016/j.icheatmasstransfer.2006.12.007.

26. Chai, L., Xia, G., Zhou, M., Li, J. and Qi, J., "Optimum thermal design of interrupted microchannel heat sink with rectangular ribs in the transverse microchambers", ***Applied Thermal Engineering***, Vol. 51, No. 1-2, (2013), 880-889. https://doi.org/10.1016/j.applthermaleng.2012.10.037.
27. Wong, K.-C. and Lee, J.-H., "Investigation of thermal performance of microchannel heat sink with triangular ribs in the transverse microchambers", ***International Communications in Heat and Mass Transfer***, Vol. 65, No., (2015), 103-110. https://doi.org/10.1016/j.icheatmasstransfer.2015.04.011.
28. Hajmohammadi, M., Alipour, P. and Parsa, H., "Microfluidic effects on the heat transfer enhancement and optimal design of microchannels heat sinks", ***International Journal of Heat and Mass Transfer***, Vol. 126, No., (2018), 808-815. https://doi.org/10.1016/j.ijheatmasstransfer.2018.06.037.
29. Topçuoğlu, K., "Trombe wall application with heat storage tank", ***Civil Engineering Journal***, Vol. 5, No. 7, (2019), 1477-1489. DOI: 10.28991/cej-2019-03091346.

Persian Abstract

چکیده

در این مقاله مدل‌سازی عددی تشکیل برفک در میکروکانال‌های با زائده‌های مستطیلی انجام شده است. میکروکانال در نادسن‌های ۰، ۰.۰۰۵ و ۰.۱ که دارای محدوده‌ی ضریب لغزشی هستند مدل‌سازی شده است. با ترکیب مدل برفک و روش جریان چند فازی اولرین، تشکیل برفک محلی و مشخصات جریان بخار آب شبیه‌سازی می‌شوند. این مقاله با مقایسه‌ی VF و همچنین تغییر دمای محلی با داده‌های تجربی صحه‌گذاری شده است. این مدل برفک، پخش چگالی برفک، پخش دما و پخش سرعت بخارآب را پیش‌بینی می‌کند. نتایج نشان می‌دهد که با گذر زمان وزن و ضخامت برفک افزایش می‌یابد. مشخصات متفاوت انتقال حرارت در منطقه‌ی لایه‌ی برفک و منطقه‌ی بخارآب توسط پخش دمایی شبیه‌سازی شده نشان داده می‌شوند. پخش سرعت شبیه‌سازی شده نشان می‌دهد که سرعت هوا در منطقه‌ی لایه‌ی برفک نزدیک به صفر است و در منطقه‌ی بخارآب هر چقدر برفک رشد می‌کند سرعت هوا افزایش می‌یابد. دمای محلی شبیه‌سازی شده، ضخامت برفک محلی، پروفایل برفک، ضخامت برفک میانگین و وزن برفک با نتایج آزمایشگاهی تطابق دارند.